
Physical and Numerical Modelling of a Two-Well Tracer Test at the Laboratory Scale

Christophe Frippiat, Benoît Wauters, Vincent Feller, Patrick Conde,
Mohammed Talbaoui, and Alain Holeyman

Civil and Environmental Engineering, Catholic University of Louvain, Place du Levant, 1,
1348 Louvain-la-Neuve
holeyman@gce.ucl.ac.be
Tel: +32 10 47 21 12
Fax: +32 10 47 21 79

Abstract. Two-well tracer tests were performed at the laboratory scale on a large hand-compacted Bruxellian sand sample (about 2 m³), using electrical sensors buried in the soil and placed in piezometers to monitor solute concentrations. First, heterogeneity within the soil was investigated using simple one-dimensional transport experiments. Deduced permeability values showed some non-negligible variations, that had to be taken into account when interpreting two-dimensional experiments. A numerical model was then developed under Modflow®, in order to simulate two-well tracer test recovery curves under heterogeneous soil conditions. Comparison of numerical results and experimental data highlighted the need for a sufficiently refined measurement grid, as phenomena occurring in zones where fewer sensors were installed were not well simulated.

Keywords: two-well tracer test, large-scale laboratory sample, soil heterogeneity

1 Introduction

Field tracer tests are often difficult to analyse because subsoil conditions are never completely mastered and other effects, such as well bore mixing or flow field distortion near the well, are poorly controlled (Brouyère 2003). Theoretical work in order to better understand influence of these effects has been developed during the past years (Brouyère 2003, Novakowski 1992, Zlotnik and Logan 1996). But still very few laboratory investigation on large soil samples were performed in order to assess these effects under controlled conditions. This study represents a first step in this direction and shows how, given a certain soil characterization, it is possible to predict solute transport between an injection well and a recovery well.

2 Materials and Methods

2.1 Physical Model and Measurement Device

The laboratory tests were performed within an experimental device designed for transport experiments at an intermediate scale between classical laboratory col-

umn tests (about 20 centimetres) and in situ tests (from a few metres to several kilometres). The physical model consisted in a two cubic meters box (2 metres long with a 0.8 metres wide and 1.2 metres high cross-section) flanked by two water reservoirs used to impose upstream and downstream water conditions to the flow system (Fripiat et al. 2003a). The sample of Bruxellian sand was manually compacted in ten successive layers, in order to obtain a relatively homogeneous soil with about 40% total porosity. The measuring system consisted of 14 electrical sensors allowing local concentration measurements in the soil as well as in free solution (Fripiat et al. 2003b). A general linear calibration equation, compatible with Ohm's law, was used to relate electrical conductivity of the liquid phase C (expressed in μScm^{-1}) to electrical voltage drop V (in Volts) measured between the sensor electrodes

$$C = \frac{A}{V} + B \quad (1)$$

where A and B are calibration parameters. As those parameters depend on soil properties between the electrodes, they have to be determined once the sensors are in place. The tracer was a weakly concentrated salt solution (NaCl diluted in tap water). In such conditions, solution electrical conductivity is linearly related to solute concentration (at least at a constant temperature). In the next part of this paper solute concentration will be directly expressed in terms of solution electrical conductivity.

Table 1. Sensor and piezometer positions.

		C0	C1	C2	C3	C4	C5	C6	C7	C8	C9	C10	C13	Inj	Rec	P4	P5
x	M	0	2.00	2.00	0.30	0.30	0.50	0.50	0.75	1.25	1.50	1.50	1.00	0.40	1.60	1.00	1.00
y	M	-	-	-	0.25	0.55	0.55	0.25	0.4	0.4	0.25	0.55	1.00	0.40	0.40	0.20	0.60
z	M	-	-	-	0.22	0.56	0.21	0.55	0.40	0.35	0.32	0.32	-	-	-	-	-

Sensor positions as well as piezometers and wells positions in the model are summarized in Table 1. x is the distance from the model inlet, y is the distance from the left side of the sample (looking towards flow direction) and z is the elevation from sample bottom. Sensor C0 was placed in the upstream water tank, sensors C1 and C2 were placed in the downstream one, and sensor C13 recorded flux concentration in a piezometer.

2.2 Methods

Two kinds of tracer tests were performed. First, one-dimensional experiments were used to calibrate conductivity sensors and to characterize heterogeneity in the soil sample. Then, a two-well injection-recovery test was performed and analysed using data from the first experimental phase. In this section, it is proposed to briefly review the methods used to generate and to process experimental results. After having saturated the physical model with a solution at a background conductivity of $1000 \mu\text{Scm}^{-1}$ (measured at 18°C), three instantaneous stepwise variations in conductivity were successively performed: to $1300 \mu\text{Scm}^{-1}$, to $1500 \mu\text{Scm}^{-1}$ and

then back to $1000 \mu\text{Scm}^{-1}$, in order to reveal possible hysteresis effects. It can be shown that an approximate analytical solution to this problem is given by

$$\frac{C - C_0}{C_f - C_0} = \frac{1/V - 1/V_0}{1/V_f - 1/V_0} = \frac{1}{2} \left[\operatorname{erfc} \left(\frac{x - vt}{2\sqrt{\alpha_L vt}} \right) + \exp \left(\frac{x}{\alpha_L} \right) \operatorname{erfc} \left(\frac{x + vt}{2\sqrt{\alpha_L vt}} \right) \right] \quad (2)$$

where Equation 1 has been incorporated and calibration parameters dropped out. C is the conductivity [μScm^{-1}], V is the measured electrical tension [V], erfc is the complementary error function, x is the longitudinal position [m], v is the mean velocity along the travelled path [ms^{-1}], t is the time [s] and α_L is the longitudinal dispersivity [m]. Subscript 0 relates to background values and subscript f relates to stabilized final values. First, the three steps in conductivity were analysed separately. Local soil hydrodispersive parameters were deduced by least-square fitting of Equation 2 with relative measurements collected with each sensor. In a second step, experimental values recorded between breakthrough (i.e. at a theoretically constant conductivity) were used to deduce values for the calibration parameters. Then, the whole flow domain was numerically modelled and partitioned in zones of constant permeability. The flow parameters (the permeability values in the different zones) were then adjusted to produce the best fit between measurements and computed breakthrough curve. Dispersivities were kept constant and equal to the numerical grid, as calculating new values would have drastically increased the numerical difficulty of the optimisation procedure without bringing a huge improvement to solute transport modelling. The second type of tracer test involved two-dimensional effects in flow and transport and required numerical modelling to analyse concentration measurements. A background flow was created through the sample, tracer solution was injected during a short time in one well, and a constant pumping rate at the other well allowed recovery of the injected tracer 1.2 m farther.

3 One-Dimensional Tracer Test

The aim of this experimental phase is to obtain a set of calibration parameters for each sensor and to derive a description of soil macroscopic heterogeneity, in order to be able to correctly interpret any further experiment conducted within this soil sample. Fixed-head upstream and downstream conditions were respectively 0.92 m and 0.52 m, so that an average gradient of 0.2 was created in the sand sample. This high value was adopted in order to decrease experiment duration. Mean measured flow was about $8.3 \cdot 10^{-6} \text{ m}^3\text{s}^{-1}$, leading to an estimated bulk permeability of about $7.6 \cdot 10^{-5} \text{ ms}^{-1}$.

Table 2. Results of 1D-experiments and calibration procedure.

		C1	C2	C3	C4	C5	C6	C7	C8	C9	C10	C13
Step 1	v 10^{-5} ms^{-1}	4.48	4.62	2.58	2.20	3.05	1.86	3.41	2.63	2.51	2.91	3.24
	α_L cm	9.6	7.3	0.6	0.7	1.0	1.1	1.9	2.1	4.1	4.0	0.9
Step 2	v 10^{-5} ms^{-1}	4.76	4.00	2.74	2.35	3.16	1.82	3.62	2.63	2.56	2.46	3.39
	α_L cm	10.7	17.8*	0.6	0.9	2.2*	23.4*	2.4	3.7*	8.1*	9.5*	1.4
Step 3	v 10^{-5} ms^{-1}	3.18	4.02	2.82	2.28	3.21	2.028	3.89	2.81	2.86	3.06	4.01
	α_L cm	6.9	7.2	0.9	1.0	1.3	1.1	1.9	1.7	3.1	2.6	1.9
Mean	v 10^{-5} ms^{-1}	4.62	4.21	2.61	2.28	3.14	1.90	3.64	2.69	2.54	2.81	3.55
	α_L cm	8.0	7.0	0.7	0.8	1.1	1.1	2.0	2.2	3.5	4.0	1.5
Calib.	A $\text{V } \mu\text{Scm}^{-1}$	692	737	5001	3717	3714	3569	4366	3778	3686	3572	820
	B μScm^{-1}	81.4	85.6	-344	-360	-300	-317	-325	-264	-311	-269	-63

* Denoted values were not taken into account when computing mean parameters

3.1 Analytical Modelling and Sensor Calibration

Local soil hydrodispersive parameters deduced by inverse modelling are shown in Table 2. Sensors placed in the soil showed an hysteresis effect, background electrical tension values at the end of the experiment being higher than values measured before the first step. This deviation was probably due to a temperature effect, the thermal inertia of soil grains being higher than that of the flowing solution. This effect can be roughly approximated using a linear relationship

$$C_{\text{cor}} = C_{\text{meas}} (1 + K t) \quad (3)$$

where C_{cor} is the corrected conductivity, C_{meas} is the measured one and t is the time. Coefficient K was found constant for each sensor and corresponded to an increase of about 2°C of the flowing solution after the whole experiment, which agreed with temperature measurements.

Finally, conductivity levels were simulated for each sensor, using the complete injection curve. As an example, measured and theoretical breakthrough curves of sensor C7 are shown in Figure 1. Local cyclic deviations between curves could be explained via small cyclic temperature variations at the model inlet.

3.2 Numerical Modelling

A 2D numerical model of the laboratory set-up was prepared using Modflow® and MT3D®. It was composed of 200×80 cells of $1 \text{ cm} \times 1 \text{ cm}$. The flow was assumed unconfined but the effect of the unsaturated zone was not taken into account (no capillary fringe and no mass transfer above the water table). Local longitudinal dispersivity was assumed equal to the numerical grid size (1 cm). This numerical model was first used to characterize soil heterogeneity. Velocity measurements obtained from one-dimensional inverse modelling (summarized in Table 2) were used to deduce permeability values in the numerical model. The

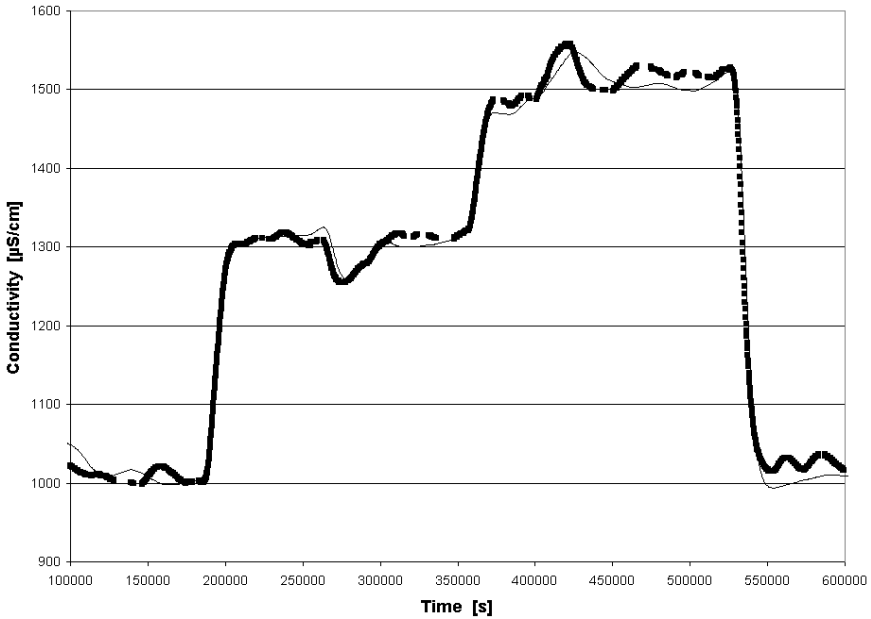


Fig. 1. Breakthrough curve at sensor C7 during 1D experimental phase. Black dots are experimental measurements and solid line is the theoretical breakthrough curve.

first step was to delineate zones within the model where permeability could be assumed constant. A reasonable, although arbitrary, choice was to take rectangular zones, each corresponding to one sensor, and placed before the sensor. Another choice could be to take zones centred on sensors. Those two delineation choices are illustrated on Figure 2.

Then, an iterative optimisation procedure was performed under Matlab®, in order to find permeability values that allowed to optimally simulate each velocity found from 1D experiment. Results in terms of estimated permeability k are shown on Table 3, as well as discrepancy between numerical simulation of the velocity v_{mod} and experimental velocity measurements v_{meas} .

In delineation case I as well as in delineation case II, one obtained a mean error on migration velocity of about 15 %, but the variance of this error seemed higher in case II.

4 Two-Well Tracer Test

4.1 Experimental Results

Fixed-head boundary conditions were kept identical as in one-dimensional experiments and the same soil sample was tested. Pumping in the recovery well was

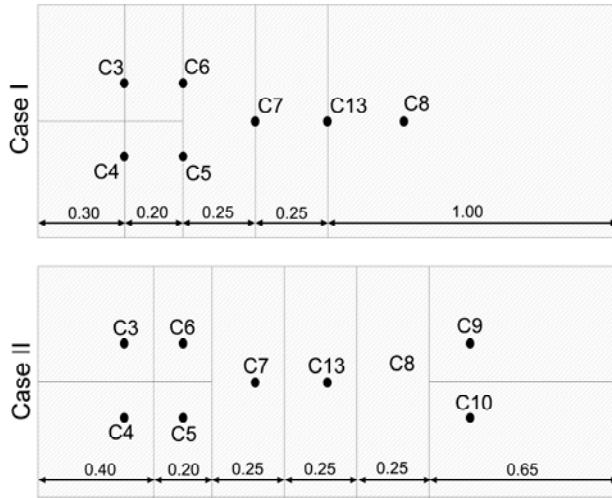


Fig. 2. Delineation of zones of constant permeability. Length measurements are in m.

Table 3. Permeability values from optimization procedure.

			C3	C4	C5	C6	C7	C13	C8	C9	C10
Case I	K	10^{-5} ms^{-1}	6.93	6.42	7.40	3.25	9.46	9.75	6.22	-	-
	v_{meas}	10^{-5} ms^{-1}	2.61	2.28	3.14	1.90	3.64	3.55	2.69	-	-
	v_{mod}	10^{-5} ms^{-1}	2.35	2.79	3.00	2.34	3.05	3.07	3.11	-	-
	Discr.	10^{-5} ms^{-1}	0.26	-0.51	0.14	-0.44	0.59	0.48	-0.42	-	-
Case II	K	10^{-5} ms^{-1}	6.20	6.31	7.17	4.66	8.37	7.81	6.43	5.66	6.54
	v_{meas}	10^{-5} ms^{-1}	2.61	2.28	3.14	1.90	3.64	3.55	2.69	2.54	2.81
	v_{mod}	10^{-5} ms^{-1}	2.41	2.62	2.77	2.47	2.81	2.87	2.92	2.84	3.11
	Discr.	10^{-5} ms^{-1}	0.20	-0.34	0.37	-0.57	0.73	0.68	-0.23	-0.30	-0.30

performed during the whole experiment at a constant rate of $1.5 \cdot 10^{-6} \text{ m}^3\text{s}^{-1}$, while injection at $1500 \mu\text{Scm}^{-1}$ was performed during 2000 s at a constant rate of $2.0 \cdot 10^{-6} \text{ m}^3\text{s}^{-1}$. As some sensors were first intended to characterize soil heterogeneity, they did not record any quantifiable information during two-well tracer test. Measurements from sensors placed upstream the injection well, as well as sensors not placed on the main flow axis, were not analysed, as it was not possible to clearly distinguish between response of the two-well system and background variations due to slight modification at the model inlet. In the next part of the text, only bell-shaped curves recorded at sensors C7, C13, C8 and at the recovery well will be analysed. In a first step, equivalent macroscopic values for permeability k_{eq} and dispersivity α_{Leq} were calculated using Modflow and are shown in Table 4. Those results are in general accordance with values deduced from 1D experiments shown on Table 2.

Table 4. 2D tracer test results.

		C7		C13			C8		Recovery				
		Exp.	I	II	Exp.	I	II	Exp.	I	II	Exp.	I	II
k_{eq}	10^{-5} ms^{-1}	7.33	-	-	7.99	-	-	5.11	-	-	7.59	-	-
α_{Leq}	cm	<1	-	-	2.5	-	-	1.2	-	-	2.5	-	-
t_{fa}	10^3 s	3.96	4.16	4.16	8.95	9.36	9.36	18.40	14.56	14.56	16.08	19.24	19.76
t_p	10^3 s	9.20	10.36	10.92	15.06	16.64	17.68	29.32	22.88	23.40	26.52	29.12	29.64
C_{max}	$\mu\text{S cm}^{-1}$	1421	1407	1419	1245	1325	1350	1283	1279	1308	1096	1115	1118

4.2 Numerical Modelling

Figure 3 shows the experimental curve at the recovery well, as well as corresponding theoretical curves in permeability cases I and II. The results were analysed considering first-arrival time t_{fa} , peak time t_p , and maximum concentration C_{max} , and are shown in Table 4. With a mean error of about 5%, maximum conductivity levels are generally well simulated, as well as arrival and peak times for sensors C7 and C13. This might mean that errors on velocities and dispersivities compensate to produce right dispersion coefficients. But C8 and recovery well shows greater differences (up to 20%) in characteristic times, which might reflect increased uncertainty on estimated permeability, due to the reduced number of sensors in this zone (as sensors C1 and C2 were not taken into account in the inverse modelling process). Moreover, adjusting dispersivity values should improve the

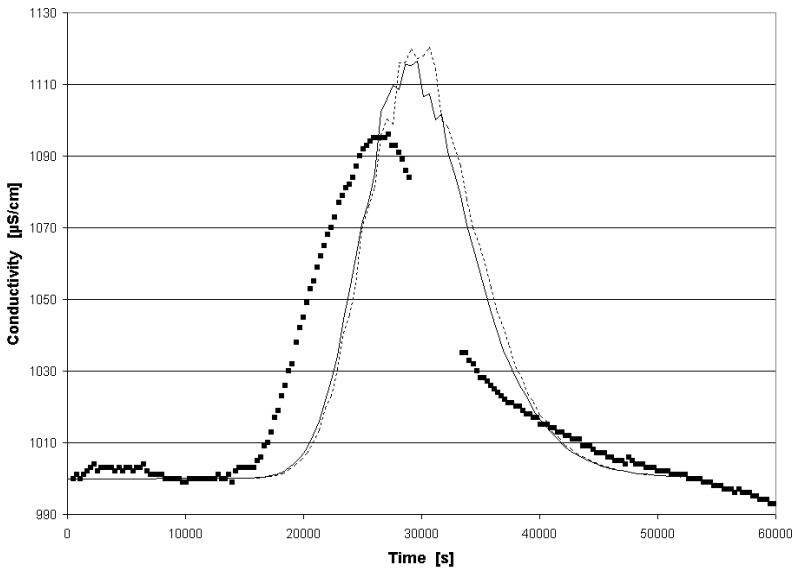


Fig. 3. Breakthrough curve at the recovery well. Black dots are experimental values, solid line corresponds to simulation I and dashed line corresponds to simulation in case II.

numerical simulation. It should also be noted at this point that no mixing effect in the injection well was included in the modelling. It is however well known that such effects may produce time delay and increased apparent dispersion (Brouyère, 2003). However, delay between first-arrival time and peak time remains relatively the same when comparing experimental data and modelling results. This might be due to the fact that estimated dispersivities in Table 4 are comparable to the local constant value used in the numerical model. Finally, numerical modelling predicted a recovery of about 97% of the solute mass injected, and integration of the experimental curve on Figure 3 provides a recovery of about 92% of the injected mass.

5 Conclusion

Results presented in this paper are only a first insight into tracer test modelling at a medium scale in the laboratory. The basic deterministic approach used here to simulate heterogeneity showed however relatively satisfactory results, at least for sensors placed in well-characterized zones, with errors between numerical modelling and measured parameters of about 5%. However, measurements near the pumping well were simulated with more difficulty, as less sensors were available in this zone. This raises the issue of correctly designing the measurement points distribution, as the electrical sensors used in the laboratory only allow one to perform local measurements. There must be a sufficient number of sensors to derive mean values that are representative of the mean behaviour of the flow system. Otherwise one has to find other characterizing tools. Future work will consist in taking permeability measurements in the physical model, so that a geostatistical characterization of soil heterogeneity can be used in a stochastic simulation of the permeability field (Gelhar and Axness 1983). This simulation will be conditioned by direct and indirect permeability measurements (Rentier et al. 2001), by head measurements and by concentration measurement.

Acknowledgements

The authors wish to thank the Laboratory of Civil Engineering of Louvain-la-Neuve, which provided helpful advice when performing physical experiments. They also would like to thank the Belgian National Fund for Scientific Research, which granted Christophe Fripiat a Research Fellowship (Ref : FC 64914).

References

- Brouyère S (2003) Modeling tracer injection and well-aquifer interactions : A new mathematical and numerical approach. *Water Resources Research* 39(3).
- Fripiat C, Servais T, Conde P, Talbaoui M, Holeyman A (2003a) Medium-scale laboratory model to assess soil contaminant dispersivity. In: *Proceedings of the 13th European Conference on Soil Mechanics and Geotechnical Engineering, August 25-28, 2003, Praha, Czech Republic.*

- Frippiat C, Renard A, Holeyman A (2003b) Development of a new electric conductivity sensor in order to characterize soil solute concentration. In: Proceedings of the 9th European Meeting of Environmental and Engineering Geophysics, August 31 - September 4, 2003, Praha, Czech Republic.
- Gelhar L W, Axness C L (1983) Three-dimensional stochastic analysis of macrodispersion in aquifers. *Water Resources Research* 19(1):161-180.
- Novakowski K S (1992) An evaluation of boundary conditions for one-dimensional solute transport. I. Mathematical development. *Water Resources Research* 28(9):2399-2410.
- Rentier C, Brouyère S, Dassargues A (2001) Integrating geophysical and tracer data for accurate solute transport modelling in heterogeneous porous media. In: Proceedings of "Groundwater Quality 2001", Sheffield (U.-K.), pp 115-118.
- Zlotnik V A, Logan J D (1996) Boundary conditions for convergent radial tracer tests and effect of well bore mixing volume. *Water Resources Research* 32(7):2323-2328.